Proceedings of the 2005 IEEE
International Conference on Robotics and Automation
Barcelona, Spain, April 2005

On the Control of the Berkeley Lower Extremity Exoskeleton (BLEEX)

H. Kazerooni, Jean-Louis Racine, Lihua Huang, and Ryan Steger
University of California, Berkeley
Berkeley, CA 94720, USA
exo@me.berkeley.edu

Abstract **− The first functional load-carrying and energetically autonomous exoskeleton was demonstrated at U.C. Berkeley, walking at the average speed of 1.3 m/s while carrying a 34 kg (75 lb) payload. Four fundamental technologies associated with the Berkeley Lower Extremity Exoskeleton (BLEEX) were tackled during the course of this project. These four core technologies include: the design of the exoskeleton architecture, control schemes, a body local area network (bLAN) to host the control algorithm and an on-board power unit to power the actuators, sensors and the computers. This article gives an overview of one of the control schemes. The analysis here is an extension of the classical definition of the sensitivity function of a system: *the ability of a system to reject disturbances* or *the measure of system robustness*. The control algorithm developed here increases the closed loop system sensitivity to its wearer's forces and torques without any measurement from the wearer (such as force, position, or electromyogram signal). The control method has little robustness to parameter variations and therefore requires a relatively good dynamic model of the system. The tradeoffs between having sensors to measure human variables and the lack of robustness to parameter variation are described.**

Index Terms **− *BLEEX, exoskeleton, human-machine, wearable robotics, control.***

I. INTRODUCTION

The primary objective of this project at U.C. Berkeley is to develop fundamental technologies associated with the design and control of energetically autonomous lower extremity exoskeletons that augment human strength and endurance during locomotion. The first field-operational lower extremity exoskeleton (commonly referred to as BLEEX) is comprised of two powered anthropomorphic legs, a power unit, and a backpack-like frame on which a variety of heavy loads can be mounted. This system provides its pilot (i.e. the wearer) the ability to carry significant loads on his/her back with minimal effort over any type of terrain. BLEEX allows the pilot to comfortably squat, bend, swing from side to side, twist, and walk on ascending and descending slopes, while also offering the ability to step over and under obstructions while carrying equipment and supplies. Because the pilot can carry significant loads for extended periods of time without reducing his/her agility, physical effectiveness increases significantly with the aid of this class of lower extremity exoskeletons. In order to address issues of field robustness and reliability, BLEEX is designed such that, in the case of power loss (e.g. from fuel exhaustion), the exoskeleton legs can be easily removed and the remainder of the device can be carried like a standard backpack.

Fig. 1 Berkeley Lower Extremity Exoskeleton (BLEEX) and pilot Ryan Steger. 1: Load occupies the upper portion of the backpack and around the Power Unit; 2: Rigid connection of the BLEEX spine to the pilot's vest; 3: Power unit and central computer occupies the lower portion of the backpack; 4: Semi-rigid vest connecting BLEEX to the pilot; 5: One of the hydraulic actuators; 6: Rigid connection of the BLEEX feet to the pilot's boots. More photographs can be found at http://bleex.me.berkeley.edu

BLEEX was first unveiled in 2004, at U.C. Berkeley's Human Engineering and Robotics Laboratory (Fig. 1). In this initial model, BLEEX offered a carrying capacity of 34 kg (75 lbs), with weight in excess of that allowance being supported by the pilot. BLEEX's unique design offers an ergonomic, highly maneuverable, mechanically robust, lightweight, and durable outfit to surpass typical human limitations. BLEEX has numerous potential applications; it can provide soldiers, disaster relief workers, wildfire fighters, and other emergency personnel the ability to carry heavy loads such as food, rescue equipment, first-aid supplies, communications gear, and weaponry, without the strain typically associated with demanding labor. Unlike unrealistic fantasy-type concepts fueled by movie-makers and science-fiction writers, the lower extremity exoskeleton conceived at Berkeley is a practical, intelligent, load-carrying robotic device. It is our vision that BLEEX will provide a versatile and realizable transport platform for mission-critical equipment.

The effectiveness of the lower extremity exoskeleton stems from the combined benefit of the human intellect provided by the pilot and the strength advantage offered by the exoskeleton; in other words, the human provides an intelligent control system for the exoskeleton while the exoskeleton actuators provide most of the strength necessary for walking. The control algorithm ensures that the exoskeleton moves in concert with the pilot with minimal interaction force between the two. The control scheme needs no direct measurements from the pilot or the human-machine interface (e.g. no force sensors between the two); instead, the controller estimates, based on measurements from the exoskeleton only, how to move so that the pilot feels very little force. This control scheme, which has never before been applied to any robotic system, is an effective method of generating locomotion when the contact location between the pilot and the exoskeleton is unknown and unpredictable (i.e. the exoskeleton and the pilot are in contact in variety of places). This control method differs from compliance control methods employed for upper extremity exoskeletons [4], [7], and [8], and haptic systems [5], and [6] because it requires no force sensor between the wearer and the exoskeleton.

The basic principle for the control of BLEEX rests on the notion that the exoskeleton needs to shadow the wearer's voluntary and involuntary movements quickly, and without delay. This requires a high level of sensitivity in response to all forces and torques on the exoskeleton, particularly the forces imposed by the pilot. Addressing this need involves a direct conflict with control science's goal of minimizing system sensitivity in the design of a closed loop feedback system. If fitted with a low sensitivity, the exoskeleton would not move in concert with its wearer. We realize, however, that maximizing system sensitivity to external forces and torques leads to a loss of robustness in the system.

Taking into account this new approach, our goal was to develop a control system for BLEEX with high sensitivity. We were faced with two realistic concerns; the first was that an exoskeleton with high sensitivity to external forces and torques would respond to other external forces not initiated by its pilot. For example, if someone pushed against an exoskeleton that had high sensitivity, the exoskeleton would move just like the way it would move in response to the forces from its pilot. Although the fact that it does not stabilize its behavior on its own in response to other forces may sound like a serious problem, if it did (e.g. using a gyro), the pilot would receive motion from the exoskeleton unexpectedly and would have to struggle with it to avoid unwanted movement. The key to stabilizing the exoskeleton and preventing it from falling in response to external forces depends on the pilot's ability to move quickly (e.g. step back or sideways) to create a stable situation for himself and the exoskeleton. For this, a very wide control bandwidth is needed so the exoskeleton can respond to both pilot's voluntary and involuntary movements (i.e. reflexes).

The second concern is that systems with high sensitivity to external forces and torques are not robust to variations and therefore the precision of the system performance will be proportional to the precision of the exoskeleton dynamic model. Although this is a serious drawback, we have accepted it as unavoidable. Nevertheless, various experimental systems in our laboratory have proved the overall effectiveness of the control method in shadowing the pilot's movement.

II. Previous Work

In our research work at Berkeley, we have divided the technology associated with human power augmentation into lower extremity exoskeletons and upper extremity exoskeletons. The reason for this was two-fold; firstly, we could envision a great many applications for either a stand-alone lower or upper extremity exoskeleton in the immediate future. Secondly, and more importantly for the separation is that the exoskeletons are in their early stages, and further research still needs to be conducted to ensure that the upper extremity exoskeleton and lower extremity exoskeleton can function well independently before we can venture an attempt to integrate them. See [10] for research work on upper extremity exoskeletons at Berkeley.

The "RoboKnee" is a powered knee brace that functions in parallel to the wearer's knee but does not transfer loads to the ground [13]. This device transfers the weight of the load onto the human skeleton (including shanks, ankles, and feet). "HAL" is a walking aid system for individuals with gait disorders [3]. Lokomat is a rehabilitation system where the patient legs are driven by the device through a predefined trajectory without any feedback from the patient [1]. Reference [12] describes a non-wearable human assisted walking device.

III. Description

A. A simple One Degree-of-Freedom (DOF) Example

The control of the exoskeleton is motivated here through the simple 1 DOF example shown in Fig. 2. This figure schematically depicts a human leg attached or interacting with a 1 DOF exoskeleton leg in a swing configuration (no interaction with the ground). For simplicity, the exoskeleton leg is shown as a rigid link pivoting about a joint and powered by a single actuator. The exoskeleton leg in this example has an actuator that produces a torque about pivot point *A*.

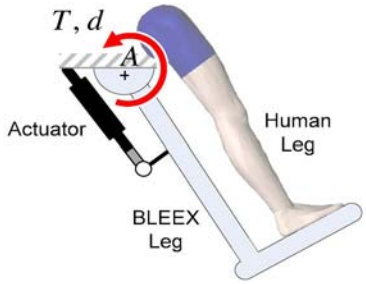

Fig. 2 Simple 1 DOF exoskeleton leg interacting with the pilot leg. The exoskeleton leg has an actuator that produces a torque *T* about the pivot point *A*. The total equivalent torque associated with all forces and torques from the pilot on the exoskeleton is represented by *d*.

Although the pilot is attached securely to the exoskeleton at the foot, other parts of the pilot leg, such as the shanks and thighs, can contact the exoskeleton and impose forces and torques on the exoskeleton leg. The location of the contacts and the direction of the contact forces (and sometimes contact torques) vary and are therefore considered unknown values in this analysis. In fact, one of the primary objectives in designing BLEEX was to ensure a pilot's unrestricted interaction with BLEEX. The equivalent torque on the exoskeleton leg, resulting from the pilot's applied forces and torques, is represented by d.

In the absence of gravity, (1) and the block diagram of Fig. 3 represent the dynamic behavior of the exoskeleton leg regardless of any kind of internal feedback the actuator may have.

$$v = G\,r + S\,d \tag{1}$$

where G represents the transfer function from the actuator input, r, to the exoskeleton angular velocity, v (actuator dynamics are included in G). In the case where multiple actuators produce controlled torques on the system, r is the vector of torques imposed on the exoskeleton by the actuators. The form of G and the type of internal feedback for the actuator is immaterial for the discussion here. Also bear in mind the omission of the Laplace operator in all equations for the sake of compactness.

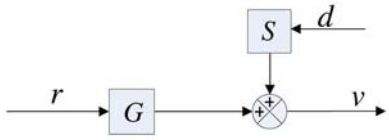

Fig. 3 The exoskeleton's angular velocity is shown as a function of the input to the actuators and the torques imposed by the pilot onto the exoskeleton.

The exoskeleton velocity, as shown by (1), is affected by forces and torques from its pilot. The sensitivity transfer function S, represents how the equivalent human torque affects the exoskeleton angular velocity. S maps the equivalent pilot torque, d, onto the exoskeleton velocity, v. If the actuator already has some sort of primary stabilizing controller, the magnitude of S will be small and the exoskeleton will only have a small response to the imposed forces and torques from the pilot or any other source. For example, a high gain velocity controller in the actuator results in small S, and consequently a small exoskeleton response to forces and torques. Also, non-backdrivable actuators (e.g. large transmission ratios or servo-valves with overlapping spools) result in a small S which leads to a correspondingly small response to pilot forces and torques.

Note that d (resulting torque from pilot on the exoskeleton) is not an exogenous input; it is a function of the pilot dynamics and variables such as position and velocity of the pilot and the exoskeleton legs. These dynamics change from person to person, and within a person as a function of time and posture. We will add these dynamics to our analysis in later paragraphs, but it is unrelated to the purpose of current discussion. We also assume that d is only from the pilot and does not include any other external forces and torques.

The objective is to increase exoskeleton sensitivity to pilot forces and torques through feedback but *without* measuring d. In other words, we are interested in creating a system that allows the pilot to swing the exoskeleton leg easily. Measuring d to create such systems develops several hard, but ultimately solvable problems in the control of a lower extremity exoskeleton. Some of those problems are briefly described below:

1) Depending on the architecture and the design of the exoskeleton, one needs to install several force and torque sensors to measure all forces from the pilot on the exoskeleton because the pilot is in contact with the exoskeleton at several locations. These locations are not known in advance. For example, we have found that some pilots are interested in having braces connecting BLEEX at the shanks while some are interested in having them on the thighs. Inclusion of sensors on a leg to measure all kinds of human forces and torques may result in a system suitable for a laboratory setting but not robust enough to be deployed in the field.

2) If the BLEEX design is such that the forces and torques applied by the pilot on the exoskeleton are limited to a specified location, (e.g., the pilot foot), the sensor that measures the pilot forces and torques will also inadvertently measure other forces and torques that are not intended for locomotion. This is a major difference between measuring forces from, for example, the human hands, and measuring forces from the human lower limbs. Using our hands, we are able to impose controlled forces and torques on upper extremity exoskeletons and haptic systems with very few uncertainties. However, our lower limbs have other primary and non-voluntary functions like load support that take priority over locomotion.

3) One option we have experimented with was the installation of sensing devices for forces on the bottom of the pilot's boots, where they are connected to BLEEX. Since the force on the bottom of the pilot's boot travels from heel to toe during normal walking, several sensors are required to measure the pilot force. Ideally, we would have a matrix of force sensors between the pilot and exoskeleton feet to measure the pilot forces at all locations and at all directions, though in practice, only a few sensors could be accommodated: at the toe, ball, midfoot, and the heel. Still, this option leads to thick and bulky soles.

4) The bottoms of the human boots experience cyclic forces and torques during normal walking that lead to fatigue and eventual sensor failure if the sensor is not designed and isolated properly.

For the above reasons and our experience in the design of various lower extremity exoskeletons, it became evident that the existing state of technology in force sensing could not provide robust and repeatable measurement of the human lower limb force on the exoskeleton. Our goal then shifted to developing an exoskeleton with a large sensitivity to forces and torques from the operator using

measurements only from the exoskeleton (i.e. no sensors on the pilot or the exoskeleton interface with the pilot). Creating a feedback loop from the exoskeleton variables only, as shown in Fig. 4, the new closed-loop sensitivity transfer function is presented in (2).

$$S_{NEW} = \frac{v}{d} = \frac{S}{1+GC} \tag{2}$$

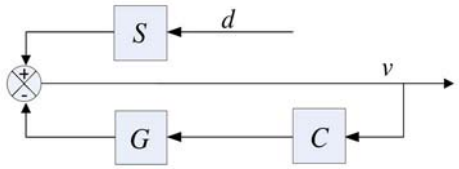

Fig. 4 Feedback control loop is added to block diagram of Fig. 3. C is the controller operating only on the exoskeleton variables.

Observation of (2) reveals that $S_{NEW} \le S$, and therefore any negative feedback from the exoskeleton, leads to an even smaller sensitivity transfer function. With respect to (2), our goal is to design a controller for a given S and G such that the closed loop response from d to v (the new sensitivity function as given by (2)) is greater than the open loop sensitivity transfer function (i.e. S) within some bounded frequency range. This design specification is given by inequality (3).

$$|S_{NEW}| > |S| \qquad \forall \omega \in (0, \omega_O) \tag{3}$$

or alternatively $|1+GC| < 1 \qquad \forall \omega \in (0, \omega_O)$ (4)

where ω_O is the exoskeleton maneuvering bandwidth.

In classical and modern control theory, every effort is made to minimize the sensitivity function of a system to external forces and torques. But for exoskeleton control, one requires a totally opposite goal: *maximize the sensitivity of the closed loop system to forces and torques*. In classical servo problems, negative feedback loops with large gains generally lead to small sensitivity within a bandwidth, which means that they reject forces and torques (usually called disturbances). However, the above analysis states that the exoskeleton controller needs a large sensitivity to forces and torques.

To achieve a large sensitivity function, we use the inverse of the exoskeleton dynamics as a positive feedback controller so that the loop gain for the exoskeleton approaches unity (slightly less than 1). Assuming positive feedback, (2) can be written as

$$S_{NEW} = \frac{v}{d} = \frac{S}{1-GC} \tag{5}$$

If C is chosen to be $C = 0.9G^{-1}$, then the new sensitivity transfer function is $S_{NEW} = 10S$ (ten times the force amplification). In general we recommend the use of positive feedback with a controller chosen as:

$$C = \left(1-\alpha^{-1}\right)G^{-1} \tag{6}$$

where α is the amplification number greater than unity (for the above example, $\alpha = 10$ led to the choice of $C = 0.9G^{-1}$). Equation (6) simply states that a positive feedback controller needs to be chosen as the inverse dynamics of the system dynamics scaled down by $(1-\alpha^{-1})$. Note that (6) prescribes the controller in the absence of unmodeled high-frequency exoskeleton dynamics. In practice, C also includes a unity gain low pass filter to attenuate the unmodeled high-frequency exoskeleton dynamics.

The above method works well if the system model (i.e. G) is well-known to the designer. If the model is not well known, then the system performance will differ greatly from the one predicted by (5), and in some cases instability will occur. The above simple solution comes with an expensive price: robustness to parameter variations. In order to get the above method working, one needs to know the dynamics of the system well. The next section discusses this tradeoff.

B. Robustness to Parameter Variations

The variation in the new sensitivity transfer function when positive feedback is used is given by (7).

$$\frac{\Delta S_{NEW}}{S_{NEW}} = \frac{\Delta S}{S} + \frac{GC}{1-GC}\frac{\Delta G}{G} \tag{7}$$

If GC is close to unity (when the force amplification number, α, is large) any parameter variation on modeling will be amplified as well. For example if the parameter uncertainty in the system is about 10%, i.e.:

$\left|\frac{\Delta G}{G}\right| = 0.10$ and $\left|\frac{\Delta S}{S}\right| = 0$, then (7) results in

$$\left|\frac{\Delta S_{NEW}}{S_{NEW}}\right| = \left|\frac{GC}{1-GC}\right| 0.10 \tag{8}$$

Now assume C is chosen such that $C = 0.9G^{-1}$.

Substituting into (8) results in $\left|\frac{\Delta S_{NEW}}{S_{NEW}}\right| = 0.90$ (9)

Equation (9) indicates that any parameter variation directly affects the system behavior. In the above example, a 10% error in model parameters results in nine times the variation in the sensitivity function. This is why model accuracy is crucial to exoskeleton control.

To get the above method working properly, one needs to understand the dynamics of the exoskeleton quite well, as the controller is heavily model based. One can see this problem as a tradeoff: the design approach described above requires no sensor (e.g. force or EMG) in the interface between the pilot and the exoskeleton; one can push and pull against the exoskeleton in any direction and at any location without measuring any variables on the interface. However, the control method requires a very good model of the system. At this time, our experiments with BLEEX have shown that this control scheme—which does not stabilize BLEEX—forces the exoskeleton to follow wide-bandwidth human maneuvers while carrying heavy loads. We have come to believe, to rephrase Friedrich Nietzsche, that *that which does not stabilize, will only make us stronger*.

C. Pilot Dynamics

There are two approaches to human muscle modeling. One is based on the investigation of the molecular or fiber range of the muscle, while the second is based on the relationship between the input and output properties of the muscle. See [15] and [16] for in-depth modeling and analysis. We have chosen the second approach and reported our preliminary work as applied to haptic systems and human power amplifiers.

In our control scheme, there is no need to include the internal components of the pilot limb model; the detailed dynamics of nerve conduction, muscle contraction, and central nervous system processing are implicitly accounted for in constructing the dynamic model of the pilot limbs. The pilot force on the exoskeleton, d, is a function of both the pilot dynamics, H, and the kinematics of the pilot limb (e.g., velocity, position or a combination thereof). In general, H is determined primarily by the physical properties of the human dynamics. Here we assume H is a nonlinear operator representing the pilot impedance as a function of the pilot kinematics.

$$d = -H(v) \tag{10}$$

The specific form of H is not known other than that it results in the human muscle force on the exoskeleton. Fig. 5 represents the closed loop system behavior when pilot dynamics is added to the block diagram of Fig. 4. Examining Fig. 5 reveals that (5), representing the new exoskeleton sensitivity function, is not affected by the feedback loop containing H.

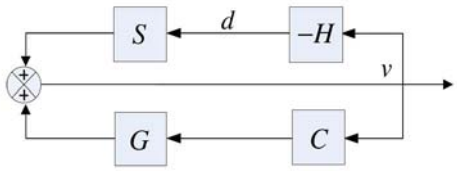

Fig. 5 This block diagram shows how an exoskeleton moves. The upper loop shows how its pilot moves the exoskeleton through applied forces. The lower loop shows how the controller drives the exoskeleton.

Fig. 5 shows an important characteristic for exoskeleton control. One can observe two feedback loops in the system. The upper feedback loop represents how forces and torques from the pilot affect the exoskeleton. The lower loop shows how the controlled feedback loop affects the exoskeleton. While the lower feedback loop is positive (potentially destabilizing), the upper feedback loop stabilizes the overall system of pilot and exoskeleton taken as a whole.

D. The Effect of Pilot Dynamics on Closed Loop Stability

How does the pilot dynamic behavior affect the exoskeleton behavior? In order to get an understanding of the system behavior in the presence of pilot dynamics we use our 1 DOF system and assume H is a linear transfer function. The stability of the system shown in Fig. 5 is decided by the closed-loop characteristic equation:

$$1 + SH - GC = 0 \tag{11}$$

In the absence of feedback controller C, the pilot carries the entire load (payload plus the weight of the exoskeleton torso). The stability in this case is decided by the characteristic equation:

$$1 + SH = 0 \tag{12}$$

Characteristic equation (12) is always stable since it represents the coupled pilot and exoskeleton behavior without any controller (i.e., when $GC = 0$). When feedback loop C is added, the closed loop characteristic equation changes from (12) to (11), and using the Small Gain Theorem, one can show that the closed loop stability is guaranteed as long as inequality (13) is satisfied:

$$|GC| < |1 + SH| \qquad \forall \omega \in (0, \infty) \tag{13}$$

According to (6), C is chosen such that $|GC| < 1$ and therefore in the absence of uncertainties, (13) is guaranteed as long as $1 \le |1 + SH|$. Unlike control methods utilized in the control of the upper extremity exoskeletons [6], the human dynamics in the control method described here has little potential to destabilize the system. Even though the feedback loop containing C is positive, the feedback loop containing H stabilizes the overall system of pilot and exoskeleton.

Example:

For a 1 DOF system, $S = G = 1/Js$, v is angular velocity, J is the moment of inertia, and s is the Laplace operator. The human impedance is modeled as $H = M_H s + C_H$ where M_H and C_H are positive quantities. If $\alpha = 10$ and the controller is chosen as $C = 0.9\,Js$, the new sensitivity function is ten times larger than the original sensitivity function:

$$S_{NEW} = \frac{v}{d} = \frac{S}{1 - GC} = 10S \tag{14}$$

The system characteristic equation when $C = 0$ is given by (15) and always results in a stable system.

$$1 + SH = \frac{(J + M_H)s + C_H}{Js} \tag{15}$$

The closed loop characteristic equation when a positive feedback loop is used is given by (16) and also results in a stable system.

$$1 + SH - GC = \frac{(0.1J + M_H)s + C_H}{Js} \tag{16}$$

Even if α is chosen as a larger number, the system in the absence of parameter uncertainties, is stable. Now suppose $\frac{\Delta J}{J} = -20\%$, i.e. $\frac{\Delta S}{S} = \frac{\Delta G}{G} = 20\%$, then the variation in new sensitivity function is,

$$\frac{\Delta S_{NEW}}{S_{NEW}} = \frac{\Delta S}{S} + \frac{GC}{1 - GC}\frac{\Delta G}{G} = 200\% \tag{17}$$

In this case, $GC = \frac{1}{0.8Js}0.9Js = \frac{9}{8}$, $S = \frac{1}{0.8Js}$, and the closed-loop characteristic polynomial is represented by (18).

$$1 + SH - GC = \frac{(10M_H - J)s + 10C_H}{8Js} \quad (18)$$

Equation (18) states that the system is unstable if $J > 10M_H$. Thus, the system is vulnerable to model parameter uncertainties. In summary, the controller discussed here is stable when worn by the pilot as long as parameter uncertainties are kept to a minimum.

IV. Implementation on BLEEX

The above discussion motivated the design philosophy using a 1 DOF system. BLEEX, as shown in Fig. 1, is a system with many degrees of freedom and therefore implementation of BLEEX control needs further attention. Each BLEEX leg has three degrees of freedom at the hip, one degree of freedom at the knee, and three degrees of freedom at the ankle. Both the flexion-extension and abduction-adduction degrees of freedom at the hip are actuated. The knee has one flexion-extension degree of freedom which is actuated. The ankle plantar-dorsi flexion (in the sagittal plane) is also actuated. The other three degrees of freedom (i.e., rotation and abduction-adduction at the ankle and rotation at the hip) are equipped with passive impedances using steel springs and elastomers. In summary, each BLEEX leg has four powered degrees of freedom: hip joint, knee joint and ankle joint in the sagittal plane and a hip abduction-adduction joint. See ----- for BLEEX preliminary design.

The pilot and BLEEX have rigid mechanical connections at the torso and the feet; everywhere else, the pilot and BLEEX have compliant or periodic contact. The connection at the torso is made using a vest, two variations of which can be seen in Fig. 1 and Fig. 6. One of the essential objectives in the design of these custom vests was to allow the distribution of the forces between BLEEX and the pilot, thereby preventing abrasion. These vests are made of several hard surfaces that are compliantly connected to each other using thick fabric. The adjustment mechanisms in the vests allow for a snug fit to the pilot. The vests include rigid plates (with hole patterns) on their backs for connection to the BLEEX torso.

The pilot's shoes or boots (Fig. 7a) attach to the BLEEX feet using a modified quick-release binding mechanism similar to snowboard bindings (Fig. 7b). A plate with the quick-release mechanism is attached to the rigid heel section of the BLEEX foot. Early versions of the BLEEX system had the pilot wearing a standard boot that has had a mating binding cleat secured to the heel. The cleat on the modified pilot boot does not interfere with normal wear when the pilot is unclipped from BLEEX. The BLEEX foot is composed of the rigid heel section with the binding mechanism and a compliant, but load bearing, toe section that begins at midfoot and extends to the toe. The BLEEX foot has a compressible rubber sole with a tread pattern that provides both shock-absorption and traction while walking. The rubber sole of the BLEEX foot contains embedded sensors, as shown in Fig. 9, that detect the trajectory of the BLEEX-ground reaction force starting from "heel-strike" to "toe-off." This information is used in the BLEEX controller to identify the BLEEX foot configuration relative to the ground.

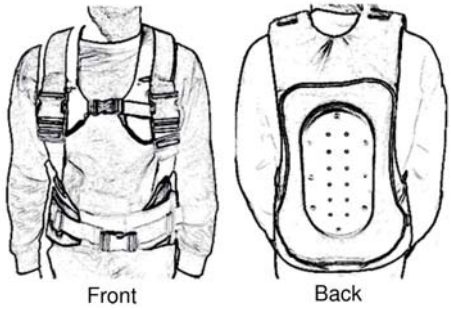

Fig. 6 The pilot vests in this figure and Fig. 1 are designed to uniformly distribute the BLEEX-pilot force on the pilot's upper body.

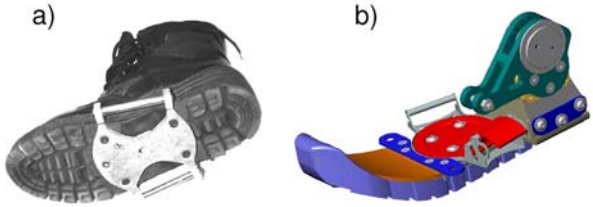

Fig. 7 Rigid attachment between a) the pilot boot and b) the BLEEX foot.

Although biomechanical studies of walking frequently identify seven or more distinct phases of the human walking gait cycle [14], for simplicity in control we consider BLEEX to have three distinct phases (shown in Fig. 8) which manifest to three different dynamic models:

Single support: one leg is in the stance configuration while another leg is in swing.

Double support: both legs are in stance configuration and situated flat on the ground.

Double support with one redundancy: both legs are in stance configuration, but one leg is situated flat on the ground while the other one is not.

Using the information from the sensors in the foot sole, the controller determines in which phase BLEEX is operating and which of the three dynamic models apply.

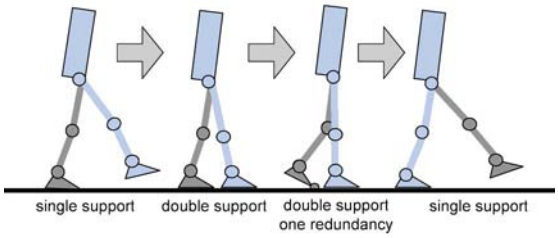

Fig. 8 Three phases of the BLEEX walking cycle.

In our initial control design process, we decoupled the control of the abduction-adduction DOF at the hip from the control of joints in the sagittal plane. This is valid because we noticed through measurements that the abduction-adduction movements during normal walking (less than 0.9 m/s or 2 mph) are rather slow. In comparison with the movements in the sagittal plane, the abduction-adduction movements can be considered quasi-static maneuvers with little dynamical affects on the rest of system. This indicates that the exoskeleton dynamics in the sagittal plane are affected only by the abduction-adduction angle and not by the abduction-adduction dynamics. For the sake of brevity,

the following sections describe the control method in the sagittal plane for a given set of abduction-adduction angles.

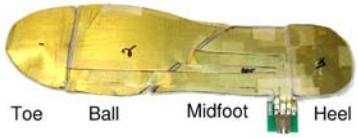

Fig. 9 The sensory system in one prototype BLEEX foot sole is composed of pressure sensitive semi-conductive rubber embedded in a polyurethane sole (Fig. 7-b). This foot measures the ground reaction force profile at four locations: toe, ball, midfoot, and heel.

A. Single Support

In the single support phase, BLEEX is modeled as the seven DOF serial link mechanism in the sagittal plane shown in Fig. 10. The dynamics of BLEEX can be written in the general form as:

$$M(\theta)\ddot{\theta} + C(\theta,\dot{\theta})\dot{\theta} + P(\theta) = T + d \tag{19}$$

where $\theta = [\theta_1 \ \ \theta_2 \ldots \theta_7]^T$ and $T = [0 \ \ T_1 \ \ T_2 \ldots T_6]^T$.

M is a 7×7 inertia matrix and is a function of θ, $C(\theta,\dot{\theta})$ is a 7×7 centripetal and Coriolis matrix and is a function of θ and $\dot{\theta}$, and P is a 7×1 vector of gravitational torques and is a function of θ only. T is the 7×1 actuator torque vector with its first element set to zero since there is no actuator associated with joint angle θ_1 (i.e. angle between the BLEEX foot and the ground). d is the effective 7×1 torque vector imposed by the pilot on BLEEX at various locations. According to (6), we choose the controller to be the inverse of the BLEEX dynamics scaled by $(1-\alpha^{-1})$, where α is the amplification number.

$$T = \hat{P}(\theta) + (1-\alpha^{-1})\left[\hat{M}(\theta)\ddot{\theta} + \hat{C}(\theta,\dot{\theta})\dot{\theta}\right] \tag{20}$$

$\hat{C}(\theta,\dot{\theta})$, $\hat{P}(\theta)$ and $\hat{M}(\theta)$ are the estimates of the Coriolis matrix, gravity vector, and the inertia matrix respectively for the system shown in Fig. 10. Note that (20) results in a 7×1 actuator torque. Since there is no actuator between the BLEEX foot and the ground, the torque prescribed by the first element of T must be provided by the pilot. Substituting T from (20) into (19) yields,

$$M(\theta)\ddot{\theta} + C(\theta,\dot{\theta})\dot{\theta} + P(\theta) = \hat{P}(\theta) + (1-\alpha^{-1})\left[\hat{M}(\theta)\ddot{\theta} + \hat{C}(\theta,\dot{\theta})\dot{\theta}\right] + d \tag{21}$$

In the limit when $M(\theta) = \hat{M}(\theta)$, $C(\theta,\dot{\theta}) = \hat{C}(\theta,\dot{\theta})$, $P(\theta) = \hat{P}(\theta)$, and α is sufficiently large, d will approach zero, meaning the pilot can walk as if BLEEX did not exist. However, it can be seen from (21) that the force felt by the pilot is a function of α and the accuracy of the estimates $\hat{C}(\theta,\dot{\theta})$, $\hat{P}(\theta)$, and $\hat{M}(\theta)$. In general, the more accurately the system is modeled, the less the human force, d, will be. In the presence of variations in abduction-adduction angles, only $P(\theta)$ in equations (19) and (20) needs to be modified.

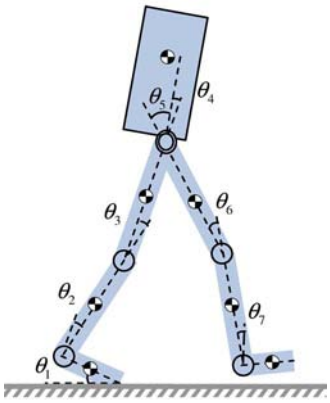

Fig. 10 Sagittal plane representation of BLEEX in the single stance phase. The "torso" includes the combined exoskeleton torso mechanism, payload, control computer, and power source.

B. Double Support

In the double support phase, both BLEEX feet are flat on the ground. The exoskeleton is modeled as two planar 3 DOF serial link mechanisms that are connected to each other along their uppermost link as shown in Fig. 11-a. The dynamics for these serial links are represented by (22) and (23).

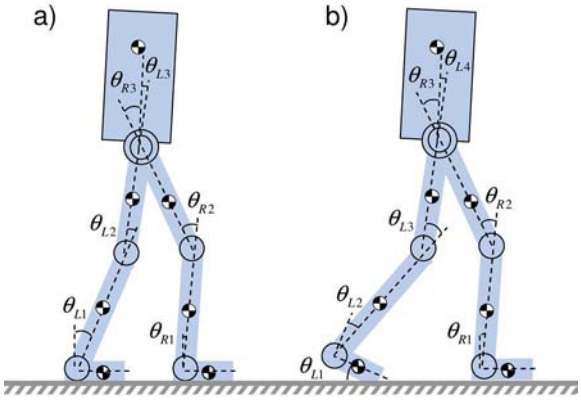

Fig. 11 Sagittal plane representation of BLEEX in a) the double support phase and b) the double support phase with one redundancy.

$$M_L(m_{TL},\theta_L)\ddot{\theta}_L + C_L(m_{TL},\dot{\theta}_L,\theta_L)\dot{\theta}_L + P_L(m_{TL},\theta_L) = T_L + d_L \tag{22}$$

$$M_R(m_{TR},\theta_R)\ddot{\theta}_R + C_R(m_{TR},\dot{\theta}_R,\theta_R)\dot{\theta}_R + P_R(m_{TR},\theta_R) = T_R + d_R \tag{23}$$

where: $\theta_L = [\theta_{L1} \ \ \theta_{L2} \ \ \theta_{L3}]^T$ and $\theta_R = [\theta_{R1} \ \ \theta_{R2} \ \ \theta_{R3}]^T$. m_{TR} and m_{TL} are effective torso masses supported by each leg and m_T is the total torso mass such that:

$$m_T = m_{TR} + m_{TL} \tag{24}$$

The contributions of m_T on each leg (i.e., m_{TL} and m_{TR}) are chosen as functions of the location of the torso center of mass relative to the locations of the ankles such that:

$$\frac{m_{TR}}{m_{TL}} = \frac{x_{TL}}{x_{TR}} \tag{25}$$

where x_{TL} is the horizontal distance between the torso center of mass and the left ankle, and x_{TR} is the horizontal distance between the torso center of mass and the right ankle. For example, if the center of mass of the torso is located directly above the right leg, then $m_{TL} = 0$ and $m_{TR} = m_T$. Similar to the single stance phase, the controllers are chosen such that

$$T_L = \hat{P}_L(m_{TL}, \theta_L) + (1 - \alpha^{-1})\left[\hat{M}_L(m_{TL}, \theta_L)\ddot{\theta}_L + \hat{C}_L(m_{TL}, \theta_L, \dot{\theta}_L)\dot{\theta}_L\right] \quad (26)$$

$$T_R = \hat{P}_R(m_{TR}, \theta_R) + (1 - \alpha^{-1})\left[\hat{M}_R(m_{TR}, \theta_R)\ddot{\theta}_R + \hat{C}_R(m_{TR}, \theta_R, \dot{\theta}_R)\dot{\theta}_R\right] \quad (27)$$

Needless to say, (25) is valid only for quasi-static conditions, where the accelerations and velocities are small. This is in fact the case, since in the double support phase, both legs are on the ground and BLEEX's angular acceleration and velocities are quite small. This allows us to simplify (26) and (27) during slow walking by removing all terms except the estimates of the gravitational vectors.

C. Double Support with One Redundancy

Double support with one redundancy is modeled as a 3 DOF serial link mechanism for the stance leg with the foot flat on the ground and a 4 DOF serial link mechanism for the stance leg that is not completely on the ground (Fig. 11-b). Each serial link supports a portion of the torso weight. The dynamics for these serial links are represented by (28) and (29), where in the specific moment shown in Fig. 11-b, the left leg has four degrees of freedom and the right leg has three degrees of freedom.

$$M_L(m_{TL}, \theta_L)\ddot{\theta}_L + C_L(m_{TL}, \dot{\theta}_L, \theta_L)\dot{\theta}_L + P_L(m_{TL}, \theta_L) = T_L + d_L \quad (28)$$

$$M_R(m_{TR}, \theta_R)\ddot{\theta}_R + C_R(m_{TR}, \dot{\theta}_R, \theta_R)\dot{\theta}_R + P_R(m_{TR}, \theta_R) = T_R + d_R \quad (29)$$

where $\theta_L = [\theta_{L1} \quad \theta_{L2} \quad \theta_{L3} \quad \theta_{L4}]^T$, $\theta_R = [\theta_{R1} \quad \theta_{R2} \quad \theta_{R3}]^T$, $T_L = [0 \quad T_{L1} \quad T_{L2} \quad T_{L3}]^T$ and $T_R = [T_{R1} \quad T_{R2} \quad T_{R3}]^T$.

m_{TR} and m_{TL} are the effective torso masses supported by each leg and are computed similar to the double support case by use of (25). Utilizing (28) and (29) as dynamic models of the exoskeleton, (26) and (27) are used as controllers in this case. Clearly, the actuator torque vector associated with the leg that has four degrees of freedom (e.g. T_L in the case shown in Fig. 11, right) is a 4×1 vector. As in the single support phase, the torque prescribed by the first element of T must be provided by the pilot because there is no actuator between the BLEEX foot and the ground. As BLEEX goes through the various phases shown in Fig. 8, the sensors shown in Fig. 9 detect which leg has four degrees of freedom and which leg has three degrees of freedom. The controller then chooses the appropriate algorithm for each leg.

V. Conclusion

The Berkeley Lower Extremity Exoskeleton (BLEEX) is not a typical servo-mechanism. While providing disturbance rejection along some axes preventing motion in response to gravitational forces, BLEEX actually encourages motion along other axes in response to pilot interface forces. This characteristic requires large sensitivity to pilot forces which invalidates certain assumptions of the standard control design methodologies, and thus requires a new design approach. The controller described here uses the inverse dynamics of the exoskeleton as a positive feedback controller so that the loop gain for the exoskeleton approaches unity (slightly less than 1). Our current experiments with BLEEX have shown that this control scheme has two superior characteristics: 1) it allows for wide bandwidth maneuvers; 2) it is unaffected by changing human dynamics. The trade off is that it requires a relatively accurate model of the system. A body local area network (bLAN) to host the control algorithm is developed in [2]. Video clips which demonstrate the effectiveness of this control scheme can be found at http://bleex.me.berkeley.edu/bleex.

References

[1] Colombo, G. Jorg, M. Dietz, V., "Driven Gait Orthosis to do Locomotor Training of Paraplegic Patients", 22nd Annual International Conf. of the IEEE, EMBS, Chicago, July 23-28, 2000.

[2] Kim, S., Anwar, G., Kazerooni, H., "High-speed Communication Network for Controls with Application on the Exoskeleton", American Control Conference, Boston, June 2004.

[3] Kawamoto, H., Sankai, Y., "Power Assist System HAL-3 for gait Disorder Person", ICCHP, July 2002, Austria.

[4] Kazerooni, H., Mahoney, S., "Dynamics and Control of Robotic Systems Worn By Humans," ASME Journal of Dynamic Systems, Measurements, and Control, Vol. 113, No. 3, , Sept. 1991.

[5] Kazerooni, H., and Her, M. "The Dynamics and Control of a Haptic Interface Device," IEEE Transactions on Robotics and Automation, Vol. 10, No. 4, August 1994, pp 453-464.

[6] Kazerooni, H., Snyder, T., "A Case Study on Dynamics of Haptic Devices: Human Induced Instability in Powered Hand Controllers," AIAA J. of Guidance, Control, and Dynamics, Vol. 18, No. 1, 1995.

[7] Kazerooni, H., "Human-Robot Interaction via the Transfer of Power and Information Signals," IEEE Transactions on Systems and Cybernetics, Vol. 20, No. 2, April 1990, pp. 450-463.

[8] Kazerooni, H., Guo, J., "Human Extenders," ASME Journal of Dynamic Systems, Measurements, and Control, Vol. 115, No. 2(B), June 1993, pp 281-289.

[9] Kazerooni, H., "The extender technology at the University of California, Berkeley," Journal of the Society of Instrument and Control Engineers in Japan, Vol. 34, 1995, pp. 291-298.

[10] Kazerooni, H., "The Human Power Amplifier Technology at the University of California, Berkeley", Journal of Robotics and Autonomous Systems, Elsevier, Volume 19, 1996, pp. 179-187.

[11] Chu, A., Kazerooni, H., Zoss, A., "On the Biomimetic Design of the Berkeley Lower Extremity Exoskeleton (BLEEX)", IEEE Int. Conf. on Robotics and Automation, April 2005, Barcelona.

[12] Neuhaus, P., Kazerooni, H., "Industrial-Strength Human-Assisted Walking Robots", IEEE Robotics and Automation Magazine, Vol. 8, No. 4., December 2001, pp. 18-25.

[13] Pratt, J., Krupp, B., Morse, C., Collins, S., "The RoboKnee: An Exoskeleton for Enhancing Strength During Walking", IEEE Conf. on Robotics and Aut., New Orleans, April 2004.

[14] Rose, J., Gamble, J. G., 1994, Human Walking, Second Edition, Williams & Wilkins, Baltimore, p. 26.

[15] Wilkie, D. R., "The relation between force and velocity in human muscle", J. Physiology. K110, pp. 248-280, 1950.

[16] Winters, J. M. and Stark, L., "Analysis of fundamental human movement patterns through the use on in-depth antagonistic muscle models", IEEE Trans. on Biomed. Engr. BME32, 10, 1985.